

# **Process-Scale Modeling of Elevated Wintertime Ozone in Wyoming**

---

**Environmental Science Division**

**About Argonne National Laboratory**

Argonne is a U.S. Department of Energy laboratory managed by UChicago Argonne, LLC under contract DE-AC02-06CH11357. The Laboratory's main facility is outside Chicago, at 9700 South Cass Avenue, Argonne, Illinois 60439. For information about Argonne, see [www.anl.gov](http://www.anl.gov).

**Availability of This Report**

This report is available, at no cost, at <http://www.osti.gov/bridge>. It is also available on paper to the U.S. Department of Energy and its contractors, for a processing fee, from:

U.S. Department of Energy

Office of Scientific and Technical Information

P.O. Box 62

Oak Ridge, TN 37831-0062

phone (865) 576-8401

fax (865) 576-5728

[reports@adonis.osti.gov](mailto:reports@adonis.osti.gov)

**Disclaimer**

This report was prepared as an account of work sponsored by an agency of the United States Government. Neither the United States Government nor any agency thereof, nor UChicago Argonne, LLC, nor any of their employees or officers, makes any warranty, express or implied, or assumes any legal liability or responsibility for the accuracy, completeness, or usefulness of any information, apparatus, product, or process disclosed, or represents that its use would not infringe privately owned rights. Reference herein to any specific commercial product, process, or service by trade name, trademark, manufacturer, or otherwise, does not necessarily constitute or imply its endorsement, recommendation, or favoring by the United States Government or any agency thereof. The views and opinions of document authors expressed herein do not necessarily state or reflect those of the United States Government or any agency thereof, Argonne National Laboratory, or UChicago Argonne, LLC.

# Process-Scale Modeling of Elevated Wintertime Ozone in Wyoming

---

for  
BP America  
POC: R. Smith

by  
V.R. Kotamarthi and D.J. Holdridge  
Climate Research Section, Environmental Science Division, Argonne National Laboratory

December 2007

Work supported by BP America through U.S. Department of Energy  
contract DE-AC02-06CH11357 to Argonne National Laboratory



## Contents

Notation.....	v
Executive Summary .....	1
1 Introduction.....	3
2 Modeling Tools.....	3
3 Data Analysis.....	4
4 Model Calculations .....	8
4.1 Sensitivity to Hydrocarbons with RACM Chemistry .....	12
4.2 Results for the SAPRC Scheme.....	17
5 Conclusions.....	21
6 References.....	21

## Tables

1 Calculations used to test the model sensitivity to trace gas mixing ratios for emitted VOCs in the RACM model.....	9
2 Calculations used to test the model sensitivity to trace gas mixing ratios in the SAPRC-98 model.....	10
3 Range of meteorological variability tested .....	10

## Figures

1 Measured NO <sub>x</sub> in Boulder County, Wyoming .....	3
2 NO <sub>x</sub> versus temperature for Boulder and Daniel .....	5
3 Ozone data relationships to NO <sub>x</sub> and temperature for measurements made at Boulder.....	6
4 Measured ozone as a function of temperature at Daniel and Boulder .....	6
5 Ozone as a function of wind speed at Daniel and Boulder .....	6
6 Measured VOCs at Jonah on February 9, 2006, and February 27, 2006.....	7
7 Additional measured VOCs at Jonah on February 9, 2006, and February 27, 2006 ....	8
8 Sensitivity of model-calculated ozone to changes in surface albedo.....	11
9 Sensitivity of model-calculated ozone to changes in column ozone .....	11
10 Sensitivity of model-calculated ozone to changes in CO mixing ratio.....	13

11	Sensitivity of model-calculated ozone to changes in NO <sub>x</sub> mixing ratio .....	13
12	Sensitivity of model-calculated ozone to changes in HC <sub>3</sub> mixing ratio.....	14
13	Sensitivity of model-calculated ozone to changes in HC <sub>5</sub> and HC <sub>8</sub> mixing ratios.....	14
14	Sensitivity of model-calculated ozone to changes in ethene mixing ratio.....	15
15	Sensitivity of model-calculated ozone to changes in mixing ratios for terminal and internal alkenes .....	16
16	Sensitivity of model-calculated ozone to changes in xylene and lower reacting aromatics .....	16
17	Sensitivity of model-calculated ozone to changes in the diene family and the cresol family in the RACM scheme .....	17
18	Sensitivity of model-calculated ozone to changes in the ALK1 family, primarily ethane in the SAPRC scheme, and the ALK2 family, primarily propane .....	18
19	Sensitivity of model-calculated ozone to changes in the ALK3 family, primarily butanes in the SAPRC scheme, and the ALK5 family, primarily pentanes .....	18
20	Sensitivity of model-calculated ozone to changes in the ARO1 family, primarily toluene in the SAPRC scheme, and the ARO2 family, primarily xylene .....	19
21	Sensitivity of model-calculated ozone to changes in the CSL family, primarily cresol, in the SAPRC scheme .....	20
22	Sensitivity of model-calculated ozone to changes in the OLE1 family in the SAPRC scheme, terminal alkenes, and OLE2 family, internal alkenes .....	20

**Notation**

°C	degree(s) Celsius
DU	Dobson unit
mph	mile(s) per hour
NMHC	non-methane hydrocarbon
NO <sub>x</sub>	nitrogen oxides
ppb(v)	part(s) per billion (by volume)
ppt(v)	part(s) per trillion (by volume)
RACM	Regional Atmospheric Chemistry Mechanism
SAPRC	Statewide Air Pollution Research Center
UV	ultraviolet
VOC	volatile organic compound





## **Process-Scale Modeling of Elevated Wintertime Ozone in Wyoming**

### **Executive Summary**

Measurements of meteorological variables and trace gas concentrations, provided by the Wyoming Department of Environmental Quality for Daniel, Jonah, and Boulder Counties in the state of Wyoming, were analyzed for this project. The data indicate that highest ozone concentrations were observed at temperatures of  $-10^{\circ}\text{C}$  to  $0^{\circ}\text{C}$ , at low wind speeds of about 5 mph. The median values for nitrogen oxides ( $\text{NO}_x$ ) during these episodes ranged between 10 ppbv and 20 ppbv (parts per billion by volume). Measurements of volatile organic compounds (VOCs) during these periods were insufficient for quantitative analysis. The few available VOCs measurements indicated unusually high levels of alkanes and aromatics and low levels of alkenes. In addition, the column ozone concentration during one of the high-ozone episodes was low, on the order of 250 DU (Dobson unit) as compared to a normal column ozone concentration of approximately 300-325 DU during spring for this region. Analysis of this observation was outside the scope of this project.

The data analysis reported here was used to establish criteria for making a large number of sensitivity calculations through use of a box photochemical model. Two different VOCs lumping schemes, RACM and SAPRC-98, were used for the calculations. Calculations based on this data analysis indicated that the ozone mixing ratios are sensitive to (a) surface albedo, (b) column ozone, (c)  $\text{NO}_x$  mixing ratios, and (d) available terminal olefins. The RACM model showed a large response to an increase in lumped species containing propane that was not reproduced by the SAPRC scheme, which models propane as a nearly independent species. The rest of the VOCs produced similar changes in ozone in both schemes. In general, if one assumes that measured VOCs are fairly representative of the conditions at these locations, sufficient precursors might be available to produce ozone in the range of 60-80 ppbv under the conditions modeled.



## 1 Introduction

Measurements of ozone and its precursors in Jonah, Daniel, and Boulder Counties have shown an unexpected increase in ozone during the winter months of January and February during recent years. These months are characterized meteorologically by low ultraviolet (UV) light, temperatures near 0°C, and snow cover — and thus potentially low photochemical activity. Figure 1 shows a typical episode during 2005 with ozone mixing ratios over 100 ppb and relatively low NO<sub>x</sub> mixing ratios of about 20 ppb. The mixing ratios of several hydrocarbons were measured during such an episode. The total hydrocarbon loading (as carbon) was approximately 21.6 ppb, with most of the hydrocarbons near detection. The mixing ratio of propane was measured at 12 ppb, higher by approximately a factor of 10 than background mixing ratios in rural areas. The mixing ratio of *n*-butane was also higher than background values at over 4 ppb.

Here we use a box photochemical model constrained by the measured precursor mixing ratios with measured meteorological conditions to model predicted ozone production rates and the pathways that lead to the production of ozone in the observed mixture of trace gases. A brief description of the model below is followed by a discussion of the data available and results from the model simulations.

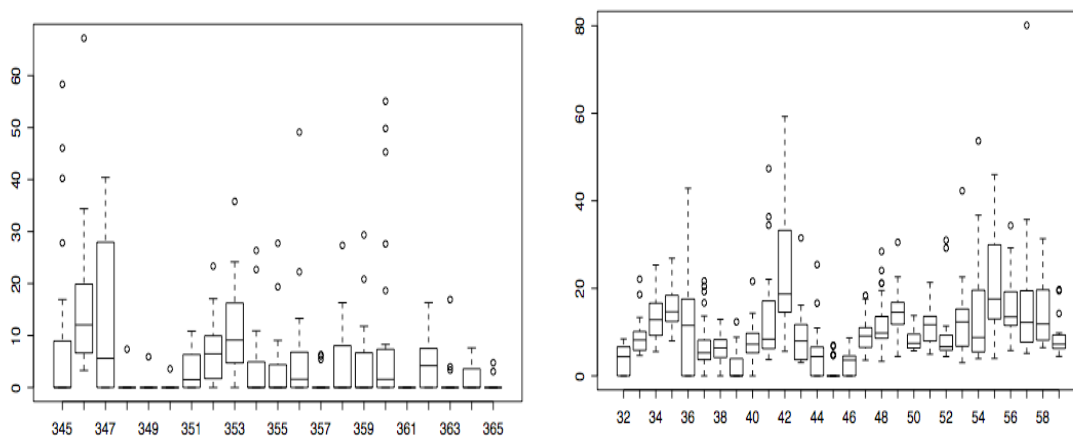


FIGURE 1 Measured NO<sub>x</sub> in Boulder County, Wyoming. Each box-whisker represents 24 hourly measurements for each day of December 2005 (left) or February 2005 (right). Concentration on the vertical axis is in ppb; the horizontal axis represents Julian days.

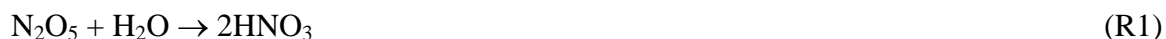
## 2 Modeling Tools

The modeling tools employed in this study include an existing photochemical box model with two different chemical schemes for VOCs. Below is a brief description of the model used.

The zero-dimensional box photochemical model has options for using two different chemical schemes. The first version, based on the University of Illinois two-dimensional zonal average model (Kotamarthi et al., 1999), has 72 species, 132 thermal reactions, and 52 photolysis rates. The base version of the model has full representation of NO<sub>x</sub>, O<sub>x</sub>, HO<sub>x</sub>, CH<sub>4</sub>, and CO

chemistry, and the reaction rates and photolytic cross section are based on the recommendations of JPL-97 (DeMore et al., 1997; and previous versions). The photolysis rate calculations are performed by using the FAST-J code of Wild et al. (2000) and updated every time step. This photolysis code was designed for calculating photolysis rates mainly in the troposphere and also to calculate the impact of clouds and aerosol layers of various types on calculated photolysis rates. The chemical integrator has the option of working either by the Gear method of Hindmarsh (1983) or the SMVGEAR II method (Jacobson and Turco, 1994), suited for vector machine computing. For the purpose of this project we used two different non-methane hydrocarbon (NMHC) schemes. The first scheme used was based on the RACM (Regional Atmospheric Chemistry Mechanism) mechanism proposed by Stockwell et al. (1997) and discussed by Kotamarthi et al. (2001). A second NMHC scheme, based on the SAPRC-98 (Carter, 2000), was also used in the calculations. The complete chemical scheme represents 79 different gas species, 214 thermal reactions, and 32 photolysis reactions, plus the heterogeneous reactions discussed below for the RACM version of the model. The SAPRC-98 version of the model also has 79 species, 190 thermal reactions, and 37 photolysis rates.

The model includes two heterogeneous reactions. The following reaction on ammonium bisulfate particles was considered a known heterogeneous reaction with a reaction probability of 0.1 and was included in all calculations:



The heterogeneous reaction rate for R1 is calculated from the reaction rate probabilities by using the following equation (Ravishankara, 1997):

$$\text{reaction rate (K)} = \omega * \text{SA} * \gamma / 4 \quad (\text{R2})$$

Here the reaction rate (K) is in  $\text{sec}^{-1}$ , while  $\omega$  is the mean molecular speed for  $\text{NO}_2$  in reaction R2 or  $\text{N}_2\text{O}_5$  in reaction R1. SA is the surface area of the aerosol particle in  $\text{cm}^2/\text{cm}^3$ , and  $\gamma$  is the reaction probability (Kotamarthi et al., 1997).

### 3 Data Analysis

Measurements of meteorological variables and trace gas concentrations, provided by the Wyoming Department of Environmental Quality for Daniel, Jonah, and Boulder Counties, were analyzed for this project. Measurements of  $\text{NO}_x$  at hourly intervals for the year 2005 in Boulder County, Wyoming, were analyzed. The median  $\text{NO}_x$  for each day of the month of December varied from 2 ppb to a high value of over 10 ppb. Extreme hourly values of over 40 ppb were measured in more than 10 instances. The median for February was nearly 10 ppbv, and extreme values of over 40 ppbv were observed on a few occasions.

To investigate the correlation between temperature and  $\text{NO}_x$  concentrations, we binned the  $\text{NO}_x$  data as a function of temperature by using temperature bins of  $10^\circ\text{C}$  width. Data for two sites Boulder and Daniel were analyzed. The lowest temperature bin was set to  $-30^\circ\text{C}$  and less, while and the highest temperature bin had temperature  $> 30^\circ\text{C}$ . The highest median  $\text{NO}_x$  values were measured during the coldest times of the year at Boulder (Figure 2). The data at Daniel

were insufficient for quantitative analysis at temperatures below  $-20^{\circ}\text{C}$ . The few available data suggest that the highest median NO<sub>x</sub> at Daniel occurred on days with temperatures between  $-10^{\circ}\text{C}$  and  $0^{\circ}\text{C}$ . The primary loss mechanism for NO<sub>x</sub> in the lower troposphere would be conversion to HNO<sub>3</sub> and subsequent deposition on snow, ice, grass, and soil. The conversion rates are slow during the colder times of year than the warm periods. Therefore, higher NO<sub>x</sub> concentrations are expected during periods with the colder temperature, under constant emission conditions. The median observed NO<sub>x</sub> on the colder days was relatively high, comparable to that of an urban location in the United States.

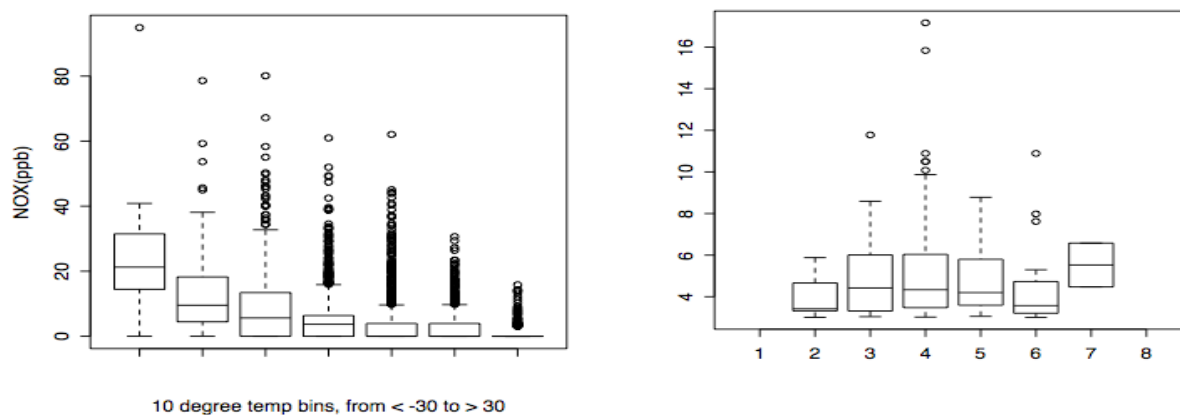


FIGURE 2 NO<sub>x</sub> versus temperature for Boulder (left) and Daniel (right). The temperature bins are of  $10^{\circ}\text{C}$  width, from  $-30^{\circ}\text{C}$  to  $> 30^{\circ}\text{C}$  (lowest to the left and highest to the right). The data from Daniel are insufficient for quantitative analysis with this type of plot; results are shown for reference only.

Measurements of ozone were made at these sites, and the relationship between NO<sub>x</sub> and ozone were explored. Figure 3 shows all ozone data for the Boulder site as a function of NO<sub>x</sub> mixing ratio (left) or temperature (right). The highest ozone mixing ratios correspond to the median observed NO<sub>x</sub> at this site of 10 ppb. At very high NO<sub>x</sub> concentrations (over 40 ppbv), the measured ozone was very low. This is expected, as high NO<sub>x</sub> is probably measured during nighttime and in the early morning, when freshly emitted NO forms a substantial portion of the NO<sub>x</sub> and ozone is titrated away from the mixture by NO. At NO<sub>x</sub> mixing ratios of 20-40 ppb, ozone varies over a wide range of values; its value is controlled by the availability of VOCs in the local atmosphere. The highest observed mixing ratios were observed at temperatures between  $-10^{\circ}\text{C}$  and  $0^{\circ}\text{C}$ , when the NO<sub>x</sub> median values were around 10 ppb (Figures 2 and 3).

The relationship of temperature to ozone was explored by using the temperature binning shown in Figure 2. Figure 4 shows the observed temperature dependence of ozone at Daniel (left) and at Boulder (right). At both sites, the highest ozone levels were measured when the temperature was between  $-10^{\circ}$  and  $0^{\circ}$ , as discussed above.

The other key meteorological parameter that controls the production of ozone is the rate of mixing in the planetary boundary layer. We used measured wind speeds as a proxy for dilution. The highest mixing ratios of ozone were observed when the wind speeds were low, in the range of 5 mph (Figure 5). Higher wind speeds correlated with higher dilution rates in the atmosphere to decrease the concentrations of ozone precursors, as well ozone itself.

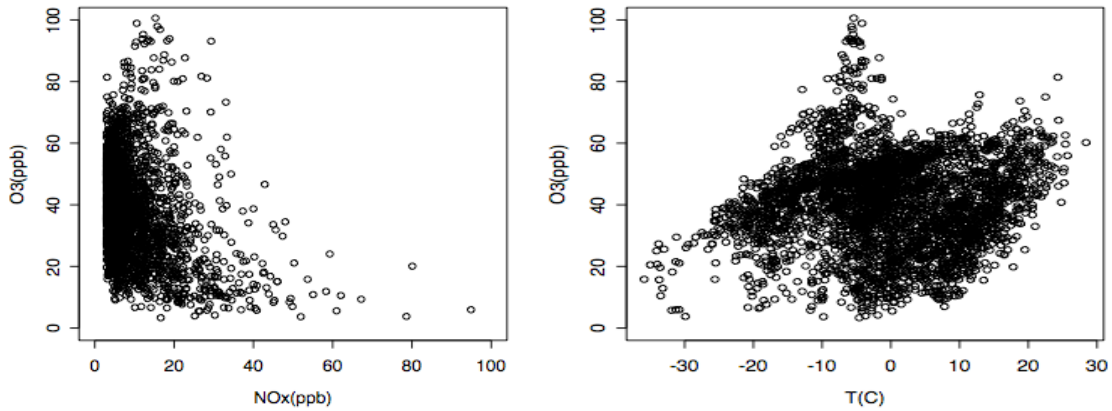


FIGURE 3 Ozone data relationships to NOx (left) and temperature (right) for measurements made at Boulder.

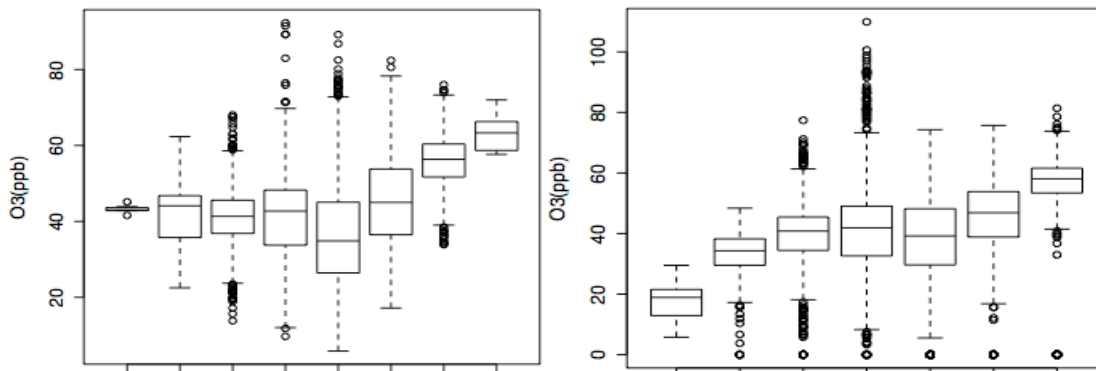


FIGURE 4 Measured ozone as a function of temperature at Daniel (left) and Boulder (right). The temperature bins (horizontal axis) are of 10°C width, from -30°C to > 30°C (lowest at left).

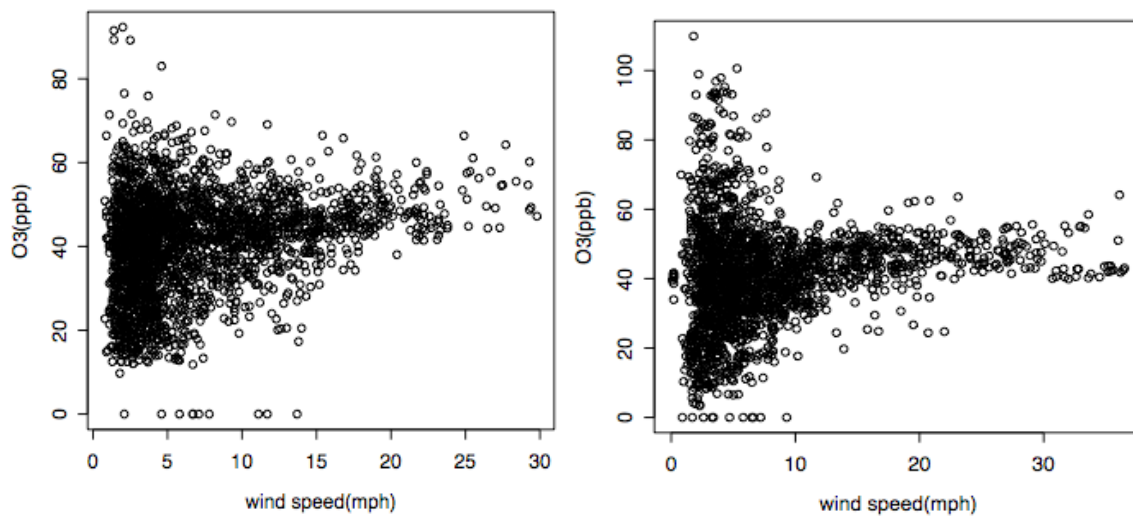


FIGURE 5 Ozone as a function of wind speed at Daniel (left) and at Boulder (right).

Unfortunately, few hydrocarbon measurements were reported for these sites. The Jonah site had measurements of VOCs on grab samples on two days in 2006, February 9 and February 27. In addition, the detection limit for several of measured VOCs was about 0.5 ppbv, quite high for gases measured at mixing ratios of approximately 10-200 pptv (parts per trillion by volume) in the background atmosphere. Consequently, we analyzed these data sets only with regard to measurements that were either much higher or much lower than background measurements for the rest of the atmosphere. Interestingly, measured values of ethane were lower than expected for a continental site, whereas the measured propane was higher by factors of 10-100 (Figure 6). Similar enhancements were noted for butane, *n*-pentane, and other alkanes. We also observed enhancement of aromatic compounds, ranging from benzene to toluene (Figure 7). Interestingly, many of the alkenes were available at very small mixing ratios and ranged over values corresponding observed continental background values.

To summarize, the highest values of ozone were observed when the temperature were between -10 and 0°C and at low wind speeds of about 5 mph. The median NO<sub>x</sub> values during these episodes ranged between 10 and 20 ppbv. Measurements of VOCs during these periods were insufficient for quantitative analysis. The few available VOCs measurements indicated unusually high concentrations of alkanes and aromatics and low concentrations of alkenes. The column ozone during one of the high-ozone episodes was also low, on the order of 250 DU, as compared to normal column ozone values of approximately 300-325 DU during springtime in this region. Analysis of this observation was outside the scope of this project.

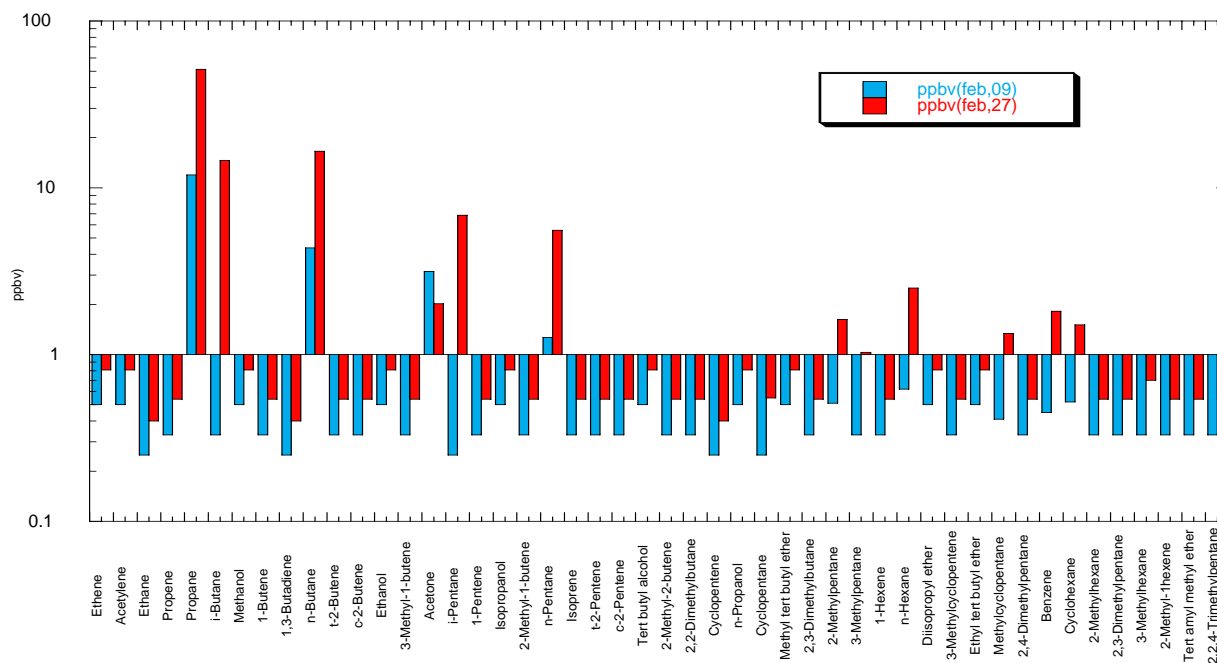


FIGURE 6 Measured VOCs at Jonah on February 9, 2006 (blue bars), and February 27, 2006 (red bars). For many compounds, the detection limit is approximately 0.5 ppbv.

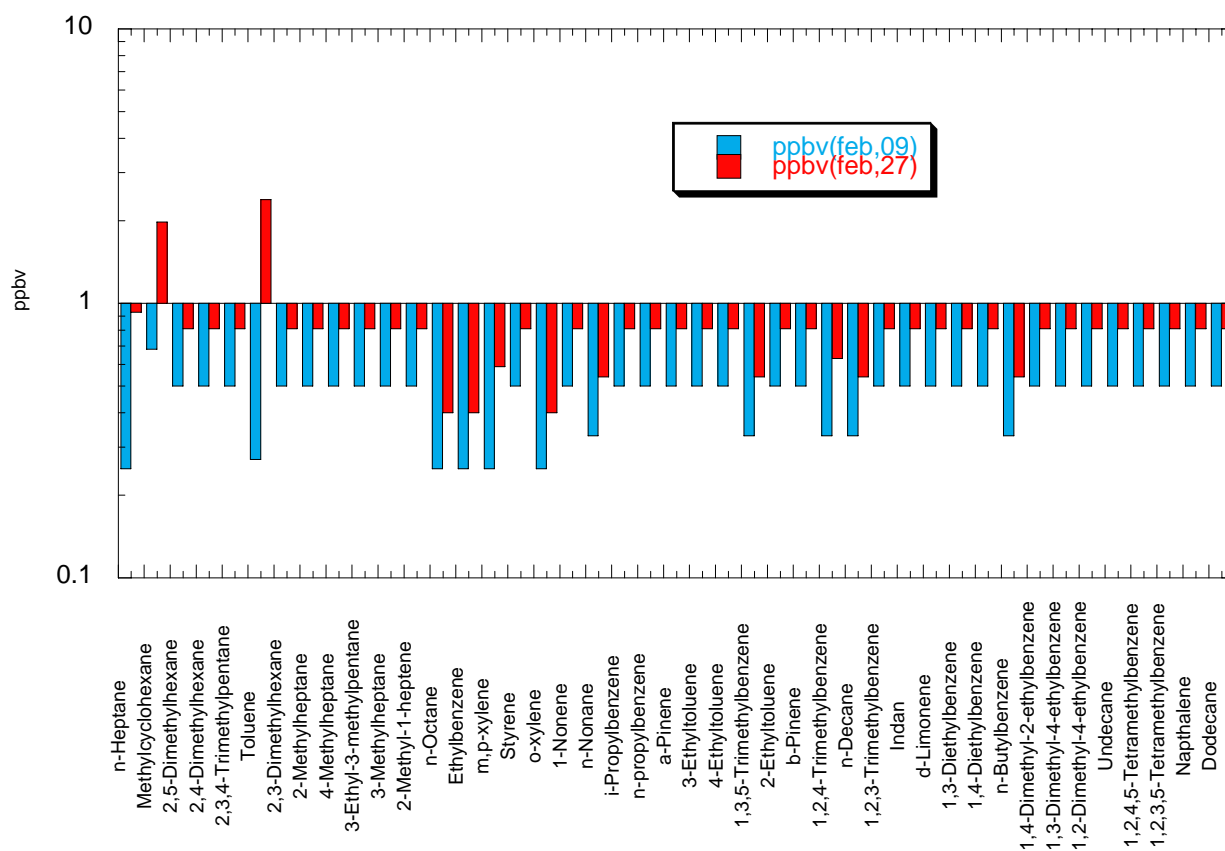


FIGURE 7 Additional measured VOCs at Jonah on February 9, 2006 (blue bars), and February 27, 2006 (red bars). For many compounds, the detection limit is approximately 0.5 ppbv.

#### 4 Model Calculations

We used the measurements reported above as a guide for establishing a matrix of calculations to test model sensitivity to the trace gas mixing ratios and meteorological conditions.

Ranges of values were explored for the two VOCs mechanisms tested, RACM and SAPRC-98. Table 1 shows the variables and ranges explored with the RACM mechanism and Table 2 shows the same for the SAPRC-98. Table 3 shows the sensitivity tests performed for the meteorological and other physical variables that are known to influence the behavior of the model. An initial set of simulations was performed to test the model sensitivity to the meteorological variables. The RACM configuration with the median concentrations of the species listed in Table 1 was used for these runs. The model was initialized with conditions at Daniel, Wyoming, longitude -110.167, latitude 42.49, and elevation of 2.1 km. Simulations were started at 0800 GMT and for Julian day 54, corresponding to February 23. Temperature was set to 273 K.



TABLE 1 Calculations used to test the model sensitivity to trace gas mixing ratios for emitted VOCs in the RACM model. Isoprene,  $\alpha$ -pinene, and d-limonene are ignored for winter conditions. ETH = ethane; HC3 = alkanes, alcohols, esters, and alkynes with OH reaction rates less than  $3.4 \times 10^{-12} \text{ cm}^3 \text{ s}^{-1}$ ; HC5 = alkanes, alcohols, esters, and alkynes with OH reaction rates between  $3.4 \times 10^{-12} \text{ cm}^3 \text{ s}^{-1}$  and  $6.8 \times 10^{-12} \text{ cm}^3 \text{ s}^{-1}$ ; HC8 = alkanes, alcohols, esters and alkynes with OH reaction rates greater than  $6.8 \times 10^{-12} \text{ cm}^3 \text{ s}^{-1}$ ; ETE = ethene; OLT = terminal alkenes; OLI = internal alkenes; TOL = toluene and less reactive aromatics; XYL = xylene and more reactive aromatics; CSL = cresol and other hydroxy substituted aromatics; DIEN = butadiene and other anthropogenic dienes. Concentrations in brackets are in ppbv. This work represents approximately 24 model runs, as “median” value cases are run only once.

	NOX	ETH	HC3	HC5	HC8	ETE	OLT	OLI	TOL	XYL	CSL	DIEN
NOX	L [10] M [15] H [40]	M [0.8]	M [0.7]	M [0.5]	M [0.5]	M [0.5]	M [0.5]	M [0.5]	M [0.5]	M [0.5]	M [0.5]	M [0.5]
ETH	M [15]	L [0.6] M [0.6] H [1.5]	M [0.7]	M [0.5]	M [0.5]	M [0.5]	M [0.5]	M [0.5]	M [0.5]	M [0.5]	M [0.5]	M [0.5]
HC3	M [15]	M [0.6]	L [0.5] M [0.7] H [15]	M [0.5]	M [0.5]	M [0.5]	M [0.5]	M [0.5]	M [0.5]	M [0.5]	M [0.5]	M [0.5]
HC5	M [15]	M [0.6]	M [0.7]	L [0.1] M [0.5] H [3.0]	M [0.5]	M [0.5]	M [0.5]	M [0.5]	M [0.5]	M [0.5]	M [0.5]	M [0.5]
HC8	M [15]	M [0.6]	M [0.7]	M [0.5]	L [0.1] M [0.5] H [1.0]	M [0.5]	M [0.5]	M [0.5]	M [0.5]	M [0.5]	M [0.5]	M [0.5]
ETE	M [15]	M [0.6]	M [0.7]	M [0.5]	M [0.5]	L [0.1] M [0.5] H [1.0]	M [0.5]	M [0.5]	M [0.5]	M [0.5]	M [0.5]	M [0.5]
OLT	M [15]	M [0.6]	M [0.7]	M [0.5]	M [0.5]	M [0.5]	L [0.1] M [0.5] H [4.0]	M [0.5]	M [0.5]	M [0.5]	M [0.5]	M [0.5]
OLI	M [15]	M [0.6]	M [0.7]	M [0.5]	M [0.5]	M [0.5]	M [0.5]	L [0.1] M [0.5] H [1.0]	M [0.5]	M [0.5]	M [0.5]	M [0.5]
TOL	M [15]	M [0.6]	M [0.7]	M [0.5]	M [0.5]	M [0.5]	M [0.5]	M [0.5]	L [0.1] M [0.5] H [1.0]	M [0.5]	M [0.5]	M [0.5]
XYL	M [15]	M [0.6]	M [0.7]	M [0.5]	M [0.5]	M [0.5]	M [0.5]	M [0.5]	M [0.5]	L [0.1] M [0.5] H [1.0]	M [0.5]	M [0.5]
CSL	M [15]	M [0.6]	M [0.7]	M [0.5]	M [0.5]	M [0.5]	M [0.5]	M [0.5]	M [0.5]	M [0.5]	L [0.1] M [0.5] H [1.0]	M [0.5]
DIEN	M [15]	M [0.6]	M [0.7]	M [0.5]	M [0.5]	M [0.5]	M [0.5]	M [0.5]	M [0.5]	M [0.5]	M [0.5]	L [0.1] M [0.5] H [1.0]

To test the sensitivity of the model to surface land cover conditions, we performed a simulation with median mixing ratios of species as shown in Table 1, setting NO<sub>x</sub> to 2 ppbv. The model was initialized with these mixing ratios and run for about 5 days for each of the calculations. Results for the first 2 days are shown in Figures 8-9. Two different albedos were tested, one corresponding to bare soil and the second corresponding to fresh snow cover. The case corresponding to fresh snow cover produced about 20 ppbv more ozone at the end of the first day than the low-albedo case.

TABLE 2 Calculations used to test the model sensitivity to trace gas mixing ratios for emitted VOCs in the SAPRC-98 model. Isoprene,  $\alpha$ -pinene, and d-limonene are ignored for winter conditions. ALK1 = ethane; ALK2 = propane, alcohols, esters, and alkynes with OH reaction rates less than  $3.4 \times 10^{-12} \text{ cm}^3 \text{ s}^{-1}$ ; ALK3 = alkanes, alcohols, esters, and alkynes with OH reaction rates between  $3.4 \times 10^{-12} \text{ cm}^3 \text{ s}^{-1}$  and  $6.8 \times 10^{-12} \text{ cm}^3 \text{ s}^{-1}$ ; ALK5 = alkanes, alcohols, esters, and alkynes with OH reaction rates greater than  $6.8 \times 10^{-12} \text{ cm}^3 \text{ s}^{-1}$ ; ETE = ethene; OLE1 = terminal alkenes; OLE2 = internal alkenes; TOL = toluene and less reactive aromatics; ARO1 = xylene and more reactive aromatics; ARO2 = cresol and other hydroxy substituted aromatics; CO = carbon monoxide. Concentrations in brackets are in ppbv. This work represents approximately 24 model runs, as “median” value cases are run only once.

	NOx	ALK1	ALK2	ALK3	ALK5	ETE	OLE1	OLE2	ARO1	ARO2	CSL	CO
NOx	L [10] M [15] H [40]	M [0.8]	M [0.7]	M [0.5]	M [0.5]	M [0.5]	M [0.5]	M [0.5]	M [0.5]	M [0.5]	M [0.5]	M [300]
ALK1	M [15]	L [0.6] M [0.6] H [1.5]	M [0.7]	M [0.5]	M [0.5]	M [0.5]	M [0.5]	M [0.5]	M [0.5]	M [0.5]	M [0.5]	M [300]
ALK2	M [15]	M [0.6]	L [0.5] M [0.7] H [15]	M [0.5]	M [0.5]	M [0.5]	M [0.5]	M [0.5]	M [0.5]	M [0.5]	M [0.5]	M [300]
ALK3	M [15]	M [0.6]	M [0.7]	L [0.1] M [0.5] H [3.0]	M [0.5]	M [0.5]	M [0.5]	M [0.5]	M [0.5]	M [0.5]	M [0.5]	M [300]
ALK5	M [15]	M [0.6]	M [0.7]	M [0.5]	L [0.1] M [0.5] H [1.0]	M [0.5]	M [0.5]	M [0.5]	M [0.5]	M [0.5]	M [0.5]	M [300]
ETE	M [15]	M [0.6]	M [0.7]	M [0.5]	M [0.5]	L [0.1] M [0.5] H [1.0]	M [0.5]	M [0.5]	M [0.5]	M [0.5]	M [0.5]	M [300]
OLE1	M [15]	M [0.6]	M [0.7]	M [0.5]	M [0.5]	M [0.5]	L [0.1] M [0.5] H [4.0]	M [0.5]	M [0.5]	M [0.5]	M [0.5]	M [300]
OLE2	M [15]	M [0.6]	M [0.7]	M [0.5]	M [0.5]	M [0.5]	M [0.5]	L [0.1] M [0.5] H [1.0]	M [0.5]	M [0.5]	M [0.5]	M [300]
ARO1	M [15]	M [0.6]	M [0.7]	M [0.5]	M [0.5]	M [0.5]	M [0.5]	M [0.5]	L [0.1] M [0.5] H [1.0]	M [0.5]	M [0.5]	M [300]
ARO2	M [15]	M [0.6]	M [0.7]	M [0.5]	M [0.5]	M [0.5]	M [0.5]	M [0.5]	M [0.5]	L [0.1] M [0.5] H [1.0]	M [0.5]	M [300]
CSL	M [15]	M [0.6]	M [0.7]	M [0.5]	M [0.5]	M [0.5]	M [0.5]	M [0.5]	M [0.5]	M [0.5]	L [0.1] M [0.5] H [1.0]	M [300]
CO	M [15]	M [0.6]	M [0.7]	M [0.5]	M [0.5]	M [0.5]	M [0.5]	M [0.5]	M [0.5]	M [0.5]	M [0.5]	L [100] M [300] H [500]

TABLE 3 Range of meteorological variability tested.

	Temp	RH	Snow Cover	Column Ozone (DU)
Temp	L M H (-10, -5, 0)	M (50%)	Y/N	M
RH	M (-5)	L M H (10%, 50%, 90%)	Y/N	M
Snow Cover	M (-5)	M(50%)	Y/N	M
Column Ozone	M (-5)	M (50%)	Y/N	L M H (250, 300, 350)

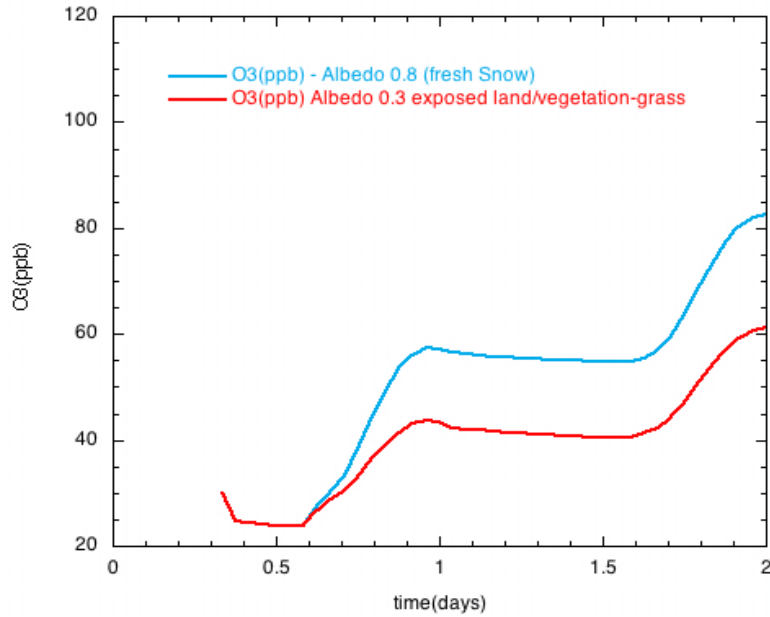


FIGURE 8 Sensitivity of model-calculated ozone to changes in surface albedo. The red line corresponds to a bare soil (albedo 0.3), and the blue line corresponds to a fresh snow cover (albedo 0.8). Column ozone was set to 350 DU, and carbon monoxide was set to 300 ppbv.

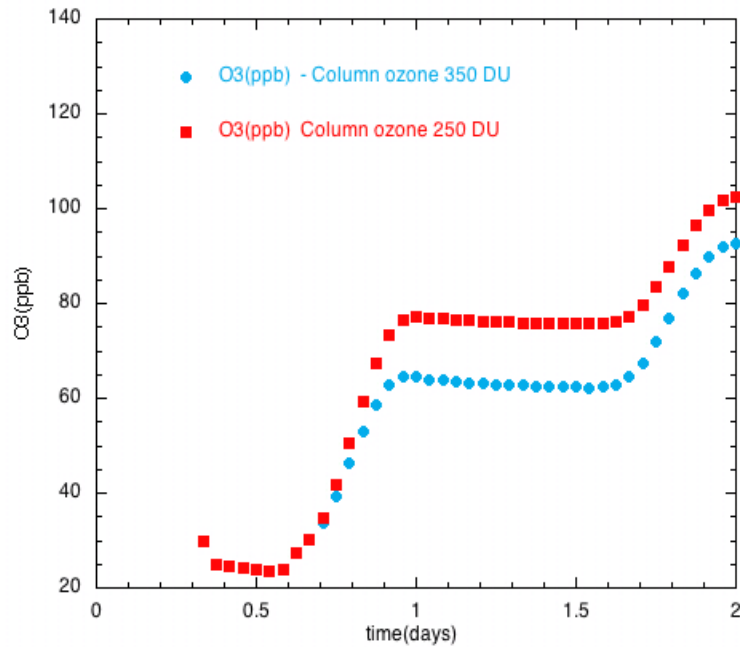


FIGURE 9 Sensitivity of model-calculated ozone to changes in column ozone. The red line corresponds to a low column ozone (250 DU), and the blue line corresponds to expected column ozone (350 DU). Albedo was set to 0.8, and carbon monoxide was set to 500 ppbv.

Two additional runs tested the sensitivity of the model to column ozone. The first run used the same median conditions as described above and NO<sub>x</sub> at 2 ppbv. The CO mixing ratio was set at 500 ppb, and two different column ozone values were tested: 250 DU and 350 DU. The latter value corresponds to the expected mean column ozone over this region during late winter and early spring. The ozone produced was similar in both cases for most of the day. The case with low column ozone had more ozone during the later part of the day, and by the end of the day this case had about 15 ppbv of excess ozone compared to the high-column-ozone case.

Another set of calculations was performed to test the sensitivity of the model to carbon monoxide concentrations (not shown in Table 1). Three different CO mixing ratios were tested: a low value of 150 ppbv (expected in background continental locations), a median value of 300 ppbv and a high value of 500 ppbv. The ozone produced in the model varied by approximately 5 ppbv with each increase in CO (Figure 10).

To test the sensitivity of the model-produced ozone to NO<sub>x</sub>, we performed three additional simulations. In all these simulations, CO was fixed at 300 ppbv, column ozone at 350 DU, and albedo at 0.8. Three different NO<sub>x</sub> mixing ratios were tested: low NO<sub>x</sub> (1 ppb), medium NO<sub>x</sub> (2 ppbv), and high NO<sub>x</sub> (10 ppbv). The high-NO<sub>x</sub> case tested here corresponds to the median NO<sub>x</sub> observed at the site during ozone episodes in February and March. The cases with NO<sub>x</sub> at 2 ppbv and 10 ppbv showed similar rates of ozone production and much higher ozone production, by about 20 ppbv at the end of the first day, than for the case with low NO<sub>x</sub> (1 ppbv). We also tested a case with the very high NO<sub>x</sub> level of 40 ppbv; the result was lower levels of ozone than with the low-NO<sub>x</sub> case shown here when all VOCs were held at their median values (Figure 11).

#### ***4.1 Sensitivity to Hydrocarbons with RACM Chemistry***

To test the sensitivity of the model to concentrations of various VOCs, we performed a series of calculations with Table 1 as a guide. In each of these calculations (presented below), the column ozone was fixed at 350 DU, the albedo was fixed at 0.8, and the mixing ratio of CO was set to 300 ppbv. The figures in this section show the results of these calculations as the concentration of the modeled species were changed over low, median, and high values, while all other hydrocarbons were held constant at the median values listed in Table 1.

Figure 12 shows the sensitivity of the model-produced ozone to changes in the lumped species HC3. In the RACM mechanism, this corresponds primarily to propane and butane. At high values of HC3, the model produced a significant increase in ozone with an increase of more than 40 ppbv at the end of the first day. Note that the SAPRC-98 mechanism results (Section 4.2) do not show this behavior. The higher sensitivity observed in the RACM scheme may be due to the lumping of propane and butane into one group and the fact that we did not weight propane and butane at the ratio RACM uses to generate the rate constant. The propane weight is unusually high and gives a very high value for this compound in the scheme. This probably leads to higher sensitivity to the high values of HC3 in the RACM mechanism. If more measurements for VOCs were available we might be able to weight them in the ratio used in generating the mechanism itself, or we might separate propane from butane to achieve proper sensitivity, as was done for the SAPRC mechanism.

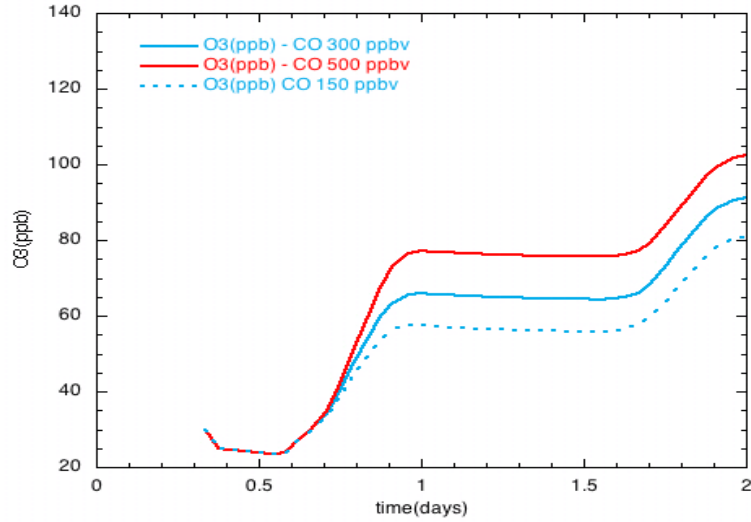


FIGURE 10 Sensitivity of model-calculated ozone to changes in CO mixing ratio. The red line corresponds to a high CO level (500 ppbv), the blue line to 300 ppbv of CO, and the dashed blue line to low CO (150 ppb).

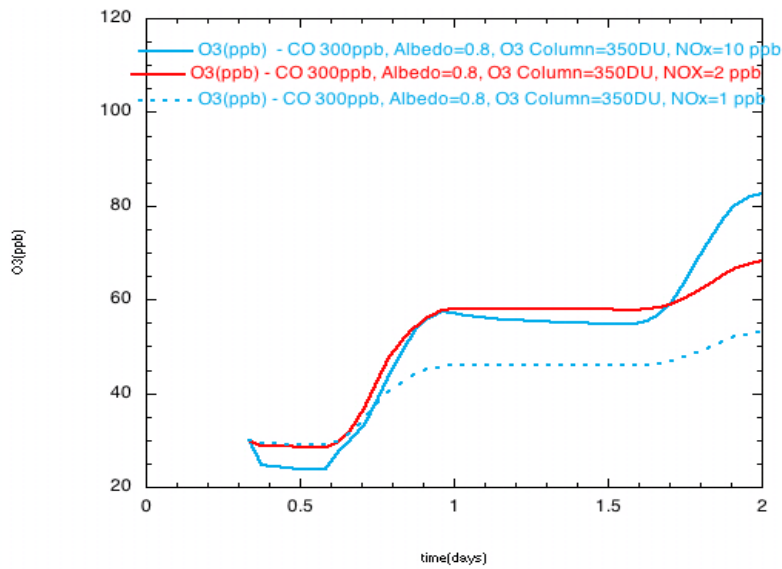


FIGURE 11 Sensitivity of model-calculated ozone to changes in NOx mixing ratio. The red line corresponds to a high NOx concentration (10 ppbv), the blue line to 2 ppbv of NOx, and the dashed blue line to low NOx (1 ppb).

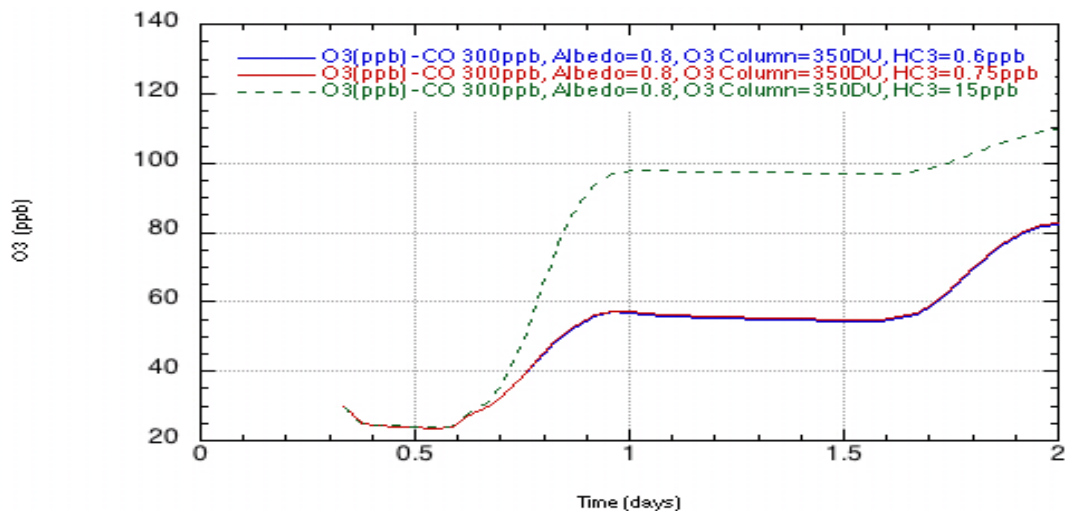


FIGURE 12 Sensitivity of model-calculated ozone to changes in HC3 mixing ratio. HC3 is primarily composed on propane and butane in the RACM mechanism. The green line corresponds to a high HC3 level (15 ppbv), the blue line to median HC3 (0.75 ppbv), and the dashed blue line to low HC3 (0.6 ppbv).

Figure 13 shows the sensitivity of model-calculated ozone to other members of the alkane family. The HC5 family consists primarily of pentane and hexane, while the HC8 family includes heptane, decane, and others. Ozone is more sensitive to the HC5 family, with approximately 10 ppb of ozone produced in excess when the HC5 mixing ratio rises from 0.5 ppbv to 3 ppbv. The highest measured mixing ratios of HC8 were low, roughly 1 ppbv.

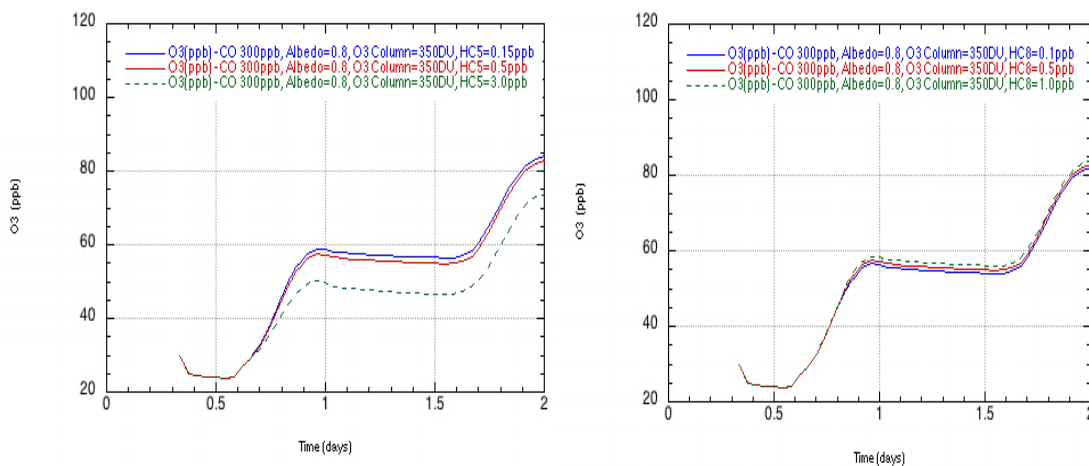


FIGURE 13 Sensitivity of model-calculated ozone to changes in HC5 (left) and HC8 (right) mixing ratios. HC5 is primarily composed of pentane and hexane, while HC8 is primarily heptane and decane in the RACM mechanism.

The sensitivity of model-calculated ozone to olefins is evaluated next. The measured values of olefins are not much higher than the background values. As a result, the changes in ozone are quite small. Figure 14 shows the changes in ozone resulting from changes in ethene from 0.1 ppb to 1 ppb. Ozone increased at the end of the day for each change in ethene, with a calculated net change of 5 ppbv for the highest ethene mixing ratio versus the lowest (0.1 ppbv).

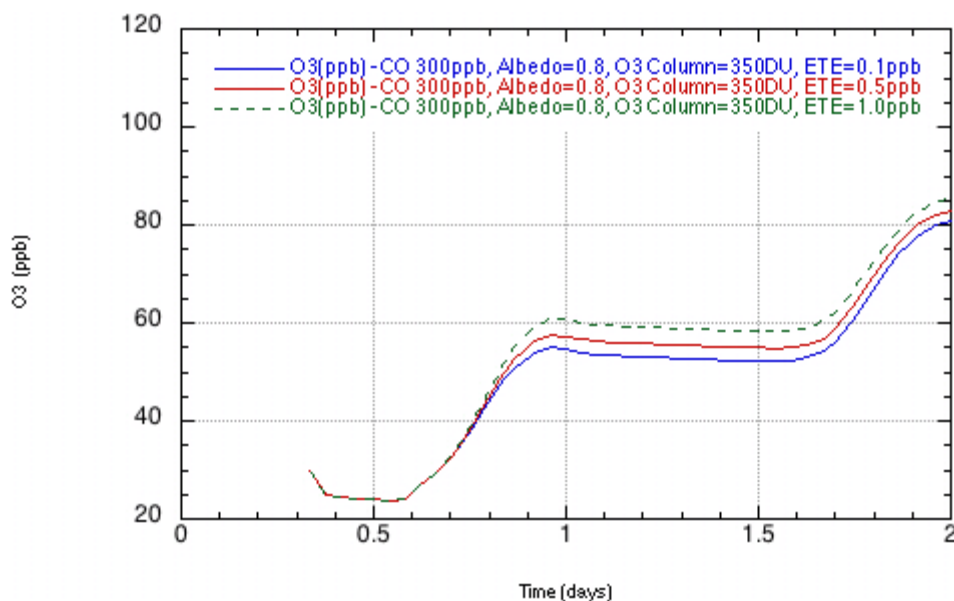


FIGURE 14 Sensitivity of model-calculated ozone to changes in ethene mixing ratio. The green line corresponds to a high ethene value (1 ppbv), the blue line to a low value (0.1 ppbv), and the red line to 0.5 ppbv.

The rest of the terminal alkenes, including propene, are considered as one lumped species named OLT in the RACM model. The model showed a large response to increased OLT and produced nearly 25 ppbv more ozone as OLT went from 0.1 ppb to 4 ppbv (Figure 15). A similar response was observed in the SAPRC-98 scheme (Section 4.2). However, the measurement detection limits of many of the terminal olefins are reported as 0.5 ppbv, and the high-end value we used (4 ppbv) might be an artifact of these rather low detection limits. The internal alkenes were varied from 0.1 ppbv to 1 ppbv and as a result showed much smaller responses to changes in the mixing ratios of OLI. Ozone is very sensitive to increases in alkenes. Better measurement of these compounds, at higher time resolution, is highly desirable for developing a better assessment of their impact in the particular situation under study here.

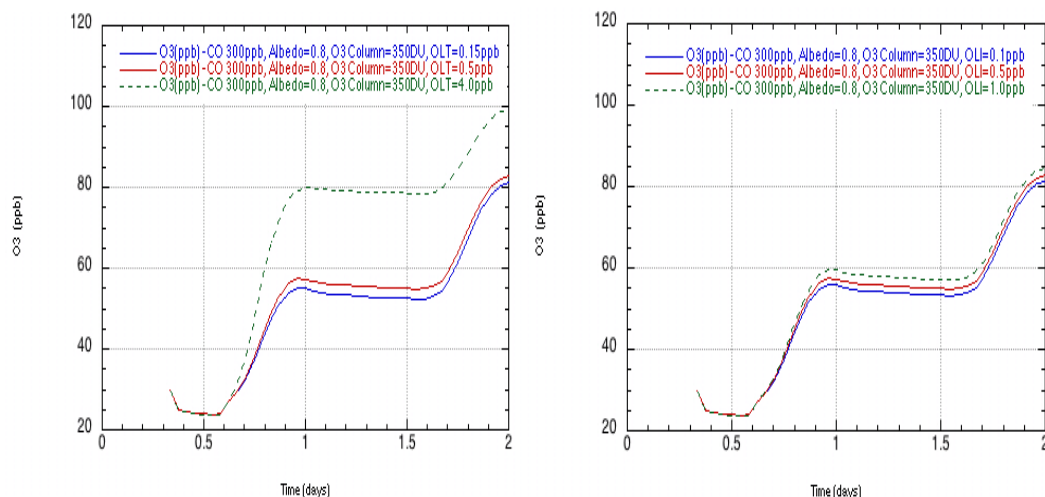


FIGURE 15 Sensitivity of model-calculated ozone to changes in mixing ratios for terminal (left) and internal (right) alkenes. The green line in the left panel corresponds to a high level of terminal alkenes (4 ppbv), the blue line to a low level (0.1 ppbv), and the red line to 0.5 ppbv. The green line in the right panel corresponds to 1 ppbv of internal alkenes, the blue line to 0.1 ppbv, and the red line to 0.5 ppbv.

We performed additional calculations to test the sensitivity of the ozone produced in the model to changes in aromatics (Figure 16). The model produced approximately 10 ppbv more ozone in response to an increase in the level of xylene and lower reacting aromatics from 0.1 ppbv to 1 ppbv.

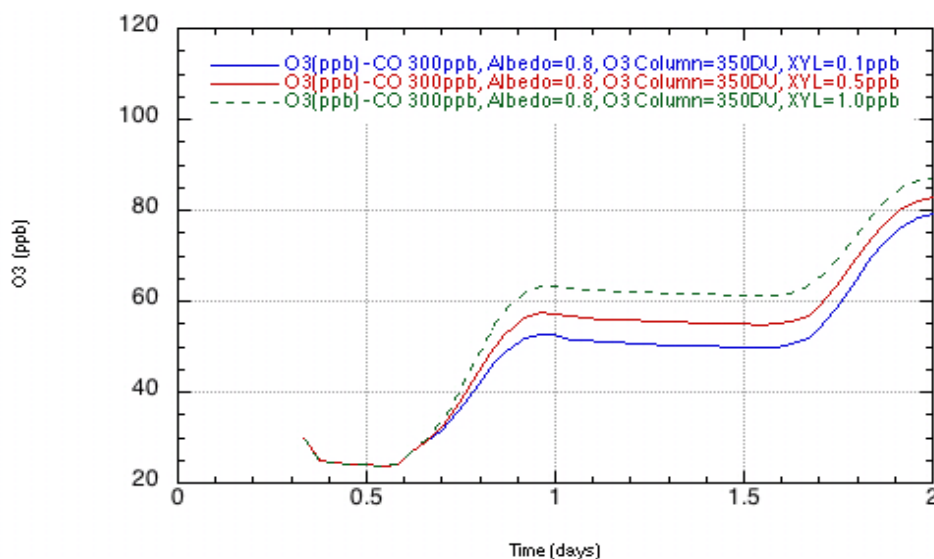


FIGURE 16 Sensitivity of model-calculated ozone to changes in xylene and lower reacting aromatics. The green line corresponds to a high level (1 ppbv), the blue line to a low level (0.1 ppbv), and the red line to 0.5 ppbv.



To complete the discussion on the calculations related to Table 1 and the RACM mechanism, the results for the diene family, which is primarily butadiene and the cresol and related hydroxy substituted aromatics, is presented in Figure 17. At the highest values of these compounds measured, we obtained an increase in ozone of less than 5 ppbv compared to the mixing ratios in the background atmosphere. In general, if we assume that measured VOCs are fairly representative of the conditions at these locations, sufficient precursor material may be available to generate ozone in the range of 60-80 ppbv under the conditions modeled.

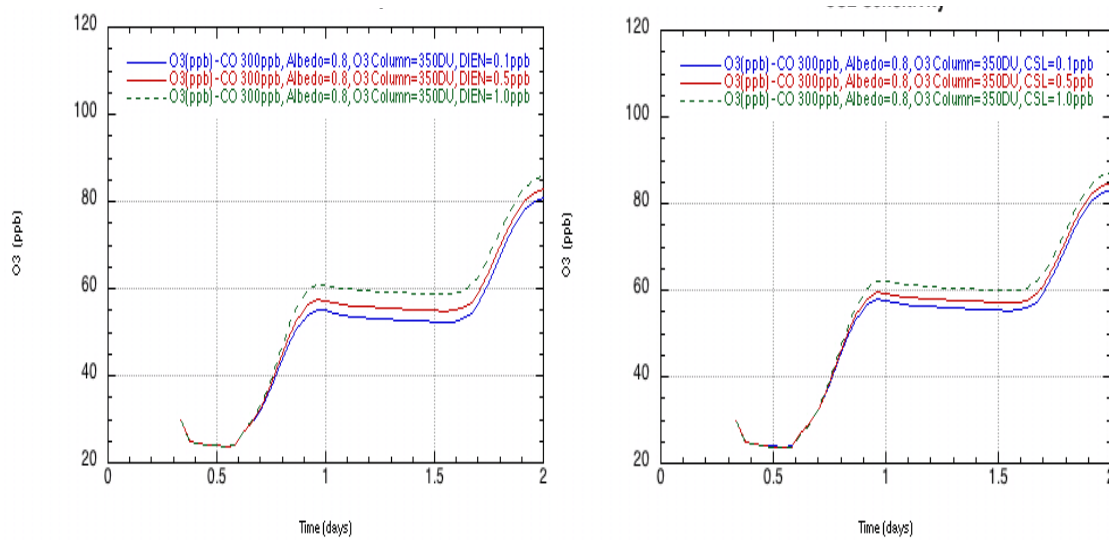


FIGURE 17 Sensitivity of model-calculated ozone to changes in the diene family (left) and the cresol family (right) in the RACM scheme. The green line corresponds to a high level (1 ppbv), the blue line to a low level (0.1 ppbv), and the red line to 0.5 ppbv.

#### 4.2 Results for the SAPRC Scheme

An analysis similar to that described above was carried out by using the SAPRC-98 chemical mechanism. All model conditions were similar to those used in the RACM model case. The VOCs scheme was switched from RACM to SAPRC-98, while the inorganic chemistry was retained as described in Section 2. The photolysis rate calculations, albedo, and column ozone were all set to the values as described above. The matrix as shown as Table 2 was used for generating the initial conditions for various lumped VOCs used in the SAPRC scheme.

The first model results from the SAPRC scheme simulations show the sensitivity of model-produced ozone to initial mixing ratios of alkanes. The SAPRC scheme has ethane (ALK1) and propane (ALK2) as separate entities. The amount of ozone produced in the ALK2 case was strikingly lower than in the HC3 case for the RACM scheme. As explained above, this could reflect RACM's use of a higher oxidation rate for HC3 than the rate for propane alone that is used for ALK2 in the SAPRC mechanism. Changes in ethane had no effect on ozone production, whereas changes in propane produced an additional 5 ppbv with the SAPRC scheme at the end of the first day (Figure 18).

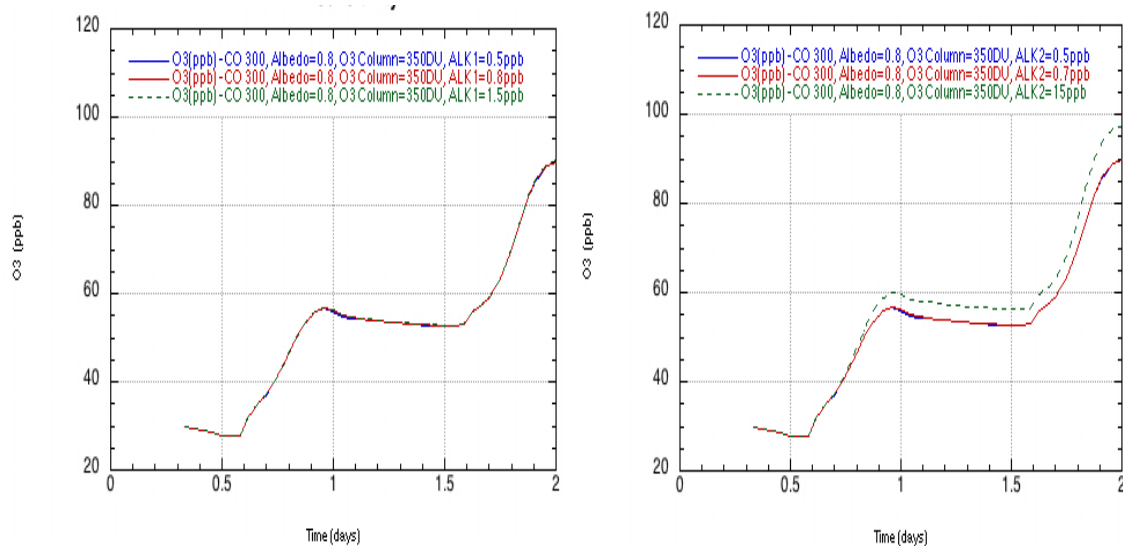


FIGURE 18 Sensitivity of model-calculated ozone to changes in the ALK1 family (left), primarily ethane in the SAPRC scheme, and the ALK2 family (right), primarily propane. In the left panel the green line corresponds to a high level of ALK1 (1.5 ppbv), the blue line to a low level (0.5 ppbv), and the red line to 0.8 ppbv. In the right panel, the green line corresponds to a high level of ALK2 (15 ppbv), the blue line to a low level (0.5 ppbv), and the red line to 0.7 ppbv.

The rest of the alkanes, lumped as ALK3 (primarily butanes) and ALK5 (primarily pentanes), also show a minor effect on ozone at their highest measured mixing ratios at this site. Changes in ozone of a few ppbv resulted as ALK3 was increased from 0.1 ppbv to 3 ppbv. Increasing ALK5 from 0.1 ppbv to 1 ppbv had an even smaller effect (Figure 19).

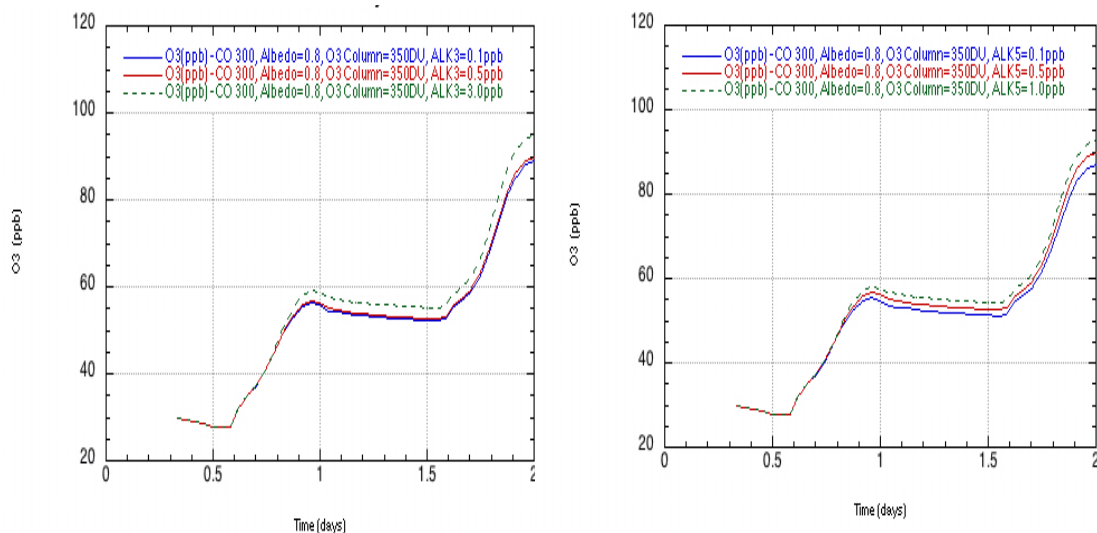


FIGURE 19 Sensitivity of model-calculated ozone to changes in the ALK3 family (left), primarily butanes in the SAPRC scheme, and the ALK5 family (right), primarily pentanes. In the left panel, the green line corresponds to a high level of ALK3 (3 ppbv), the blue line to a low level (0.1 ppbv), and the red line to 0.5 ppbv. In the right panel, the green line corresponds to a high level of ALK5 (1 ppbv), the blue line to a low level (0.1 ppbv), and the red line to 0.5 ppbv.

The SAPRC mechanism and the RACM scheme show similar increases in ozone in response to changes in aromatics. Figure 20 shows the increase in ozone due to increases in toluene and other mono alkyl benzenes (left) or xylene and related poly alkyl benzenes (right). The model is slightly more sensitive to changes in xylene than in toluene. Increases on the order of 10 ppbv (similar to RACM response) resulted when xylene increased from 0.1 ppbv to 1 ppbv.

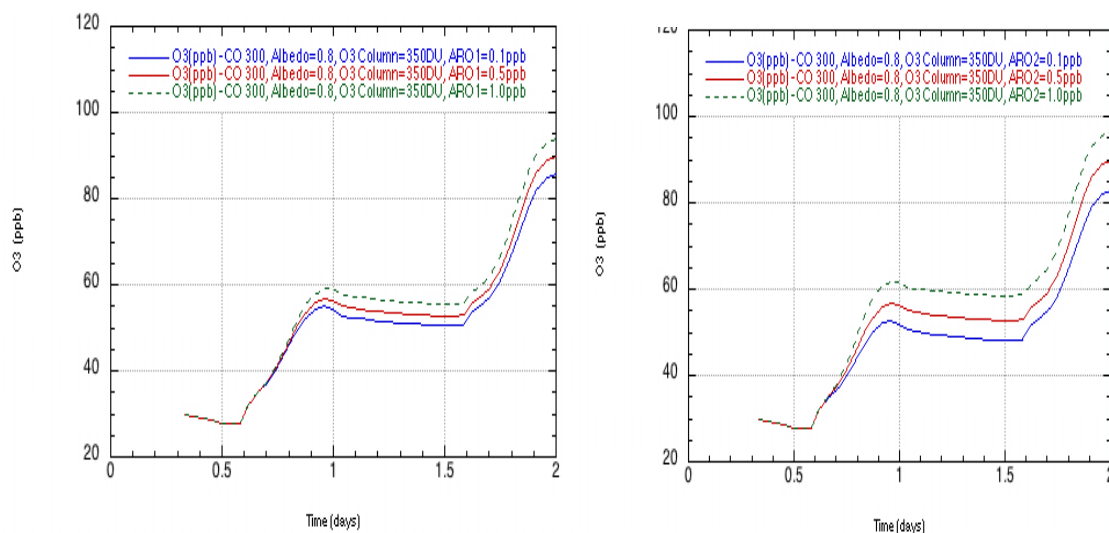


FIGURE 20 Sensitivity of model-calculated ozone to changes in the ARO1 family (left), primarily toluene in the SAPRC scheme, and the ARO2 family (right), primarily xylene. The green lines in both panels correspond to high levels (1 ppbv), the blue line to low levels (0.1 ppbv), and the red line to 0.5 ppbv.

The minor model-calculated response in terms of ozone mixing ratio for changes in cresol concentrations (Figure 21) are similar to those for RACM.

The SAPRC scheme responded identically to changes in internal and terminal alkenes (Figure 22). The response in ozone mixing ratio to changes in ethene at the measured concentrations was small and similar to the RACM result and is not shown here. A large increase in ozone resulted from increased terminal alkene (OLE1) concentrations. Again, the assumed high concentration (4 ppbv) might be an artifact of the low detection limits of the measurements. The internal alkenes show a smaller effect on ozone primarily because of smaller changes in their mixing ratios, based on reported measurements.

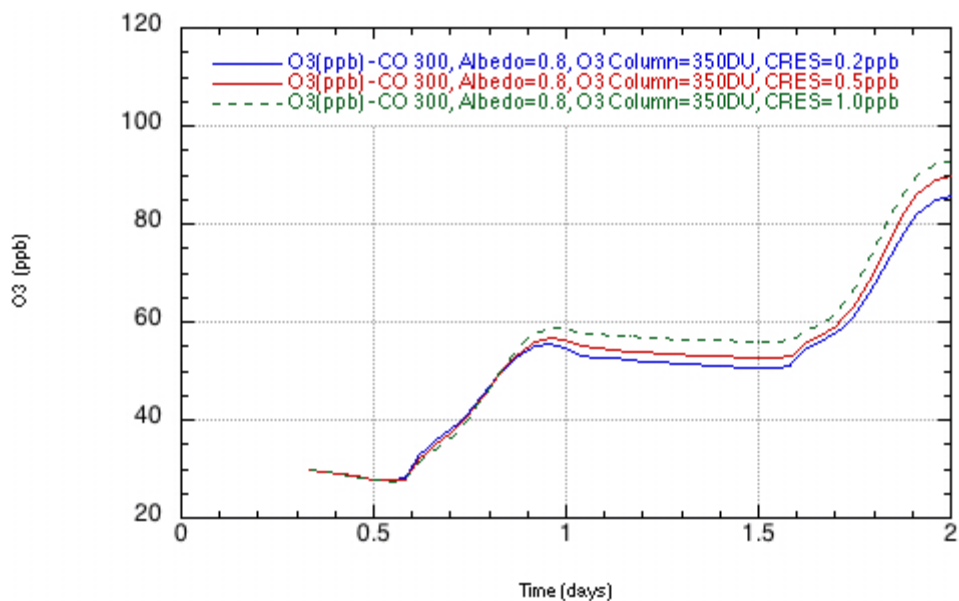


FIGURE 21 Sensitivity of model-calculated ozone to changes in the CSL (CRES) family, primarily cresol, in the SAPRC scheme. The green line corresponds to a high concentration (1 ppbv), the blue line to a low concentration (0.2 ppbv), and the red line to 0.5 ppbv.]

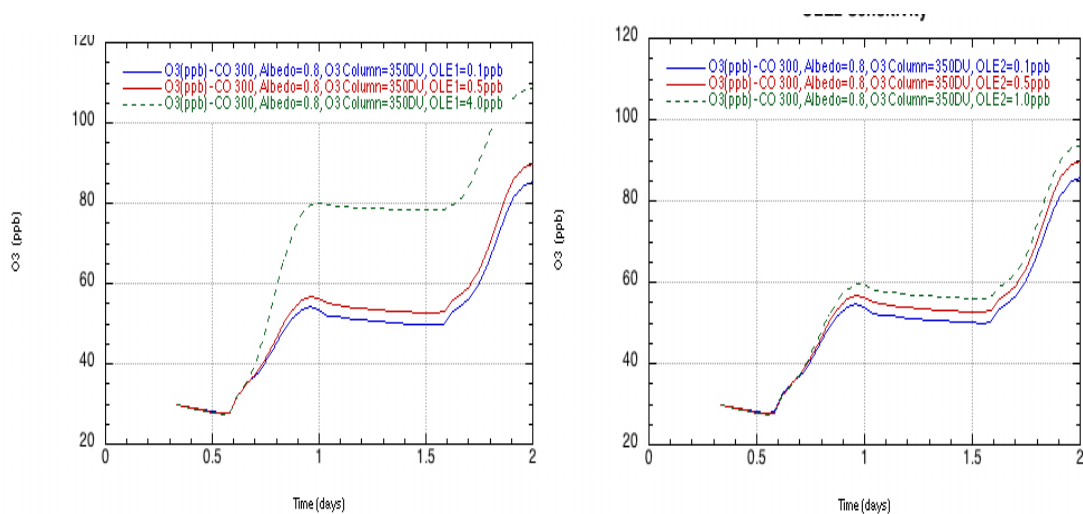


FIGURE 22 Sensitivity of model-calculated ozone to changes in the OLE1 family in the SAPRC scheme (left), terminal alkenes, and the OLE2 family (right), internal alkenes. In the left panel, the green line corresponds to a high level (4 ppbv), the blue line to a low level of OLE1 (0.1 ppbv), and the red line to 0.5 ppbv. In the right panel, the green line corresponds to a high level of OLE2 (1 ppbv), the blue line to a low level (0.1 ppbv), and the red line to 0.5 ppbv.

## 5 Conclusions

Available data from three different sites in Wyoming experiencing unusual increases in wintertime ozone were analyzed to establish criteria for making a large number of sensitivity calculations with a box photochemical model. Two different VOCs lumping schemes, RACM and SAPRC-98, were used for the calculations. The data analysis indicated that the higher ozone concentrations corresponded to temperatures in the range of -10°C to 0°C, at NO<sub>x</sub> mixing ratios of approximately 10 ppbv and low wind speeds of 5 mph. The limited numbers of VOCs measurements available indicate unusually high mixing ratios of propane and higher alkanes, as well as substantially elevated mixing ratios of aromatic compounds.

Calculations based on the data analysis presented here indicated that the ozone mixing ratios are sensitive to (a) surface albedo, (b) column ozone, (c) NO<sub>x</sub> mixing ratio, and (d) available terminal olefins. The RACM model showed a high response to an increase in a lumped species containing propane that was not reproduced by the SAPRC scheme, which models propane as a nearly independent species.

## 6 References

- Carter, W.L., 2000, *Documentation of the SAPRC-99 Chemical Mechanism for VOC Reactivity Assessment*, No. 92-329, draft prepared for the California Air Resource Board.
- DeMore, W.B., S.P. Sander, D.M. Golden, R.F. Hampson, M.J. Kurylo, C.J. Howard, A.R. Ravishankara, C.E. Kolb, and M.J. Molina, 1997, *Chemical Kinetics and Photochemical Data for Use in Stratospheric Modeling: Evaluation Number 12*, Publication 97-4, Jet Propulsion Laboratory, National Aeronautics and Space Administration, Pasadena, California.
- Hindmarsh, A.C., 1983, "ODEPACK, A Systemized Collection of ODE Solvers," in *Scientific Computing*, R. S. Stepleman et al., eds., North-Holland, Amsterdam.
- Jacobson, M.Z., and R.P. Turco, 1994, "SMVGEAR: A Sparse-Matrix Vectorized GEAR Code for Atmospheric Models," *Atmospheric Environment* 28A:273-284.
- Kotamarthi, V.R., J.M. Rodriguez, N.D. Sze, Y. Kondo, R. Pueschel, G. Ferry, S. Sandholm, G. Gregory, D. Davis, and S. Liu, 1997, "Evidence of Heterogeneous Chemistry on Sulfate Aerosols in Stratospheric Air Masses Measured in PEM-West B," *Journal of Geophysical Research* 102:28,425–28,436.
- Kotamarthi, V.R., D.J. Wuebbles, and R.A. Reck, 1999, "Effects of Non-methane Hydrocarbons on Lower Stratospheric and Upper Tropospheric 2-D Zonal Average Model Climatology," *Journal of Geophysical Research* 104:21,537-21,547.
- Kotamarthi, V.R., J.S. Gaffney, N.A. Marley, and P.V. Doskey, 2001. "Heterogeneous NO<sub>x</sub> Chemistry in the Polluted PBL," *Atmospheric Environment* 35:4489-4498.

- Ravishankara, A.R., 1997, "Heterogeneous and Multiphase Chemistry in the Troposphere," *Science* 276:1058-1065.
- Stockwell, W.R., F. Kirchner and M. Kuhn, 1997, "A New Mechanism for Regional Atmospheric Chemistry Modeling," *Journal of Geophysical Research* 102:25,847-25,879.
- Wild, O., X. Zhu, and M.J. Prather, 2000, "Fast-J: Accurate Simulation of In- and Below-Cloud Photolysis in Tropospheric Chemical Models," *Journal of Atmospheric Chemistry* 37:245-282.





**Environmental Science Division**

Argonne National Laboratory  
9700 South Cass Avenue, Bldg. 203  
Argonne, IL 60439-4843  
[www.anl.gov](http://www.anl.gov)



UChicago ►  
Argonne<sub>LLC</sub>

A U.S. Department of Energy laboratory  
managed by UChicago Argonne, LLC